THE JOURNAL OF BIOLOGICAL CHEMISTRY VOL. 291, NO. 33, pp. 17093–17101, August 12, 2016

Sialic Acid within the Glycosylphosphatidylinositol Anchor Targets the Cellular Prion Protein to Synapses*

Received for publication, April 5, 2016, and in revised form, June 16, 2016 Published, JBC Papers in Press, June 20, 2016, DOI 10.1074/jbc.M116.731117

Clive Bate[‡], William Nolan[‡], Harriet McHale-Owen[‡], and Alun Williams[§1]

From the [‡]Department of Pathology and Pathogen Biology, Royal Veterinary College, Hawkshead Lane, North Mymms, Herts AL9 7TA and the [§]Department of Veterinary Medicine, University of Cambridge, Madingley Road, Cambridge CB3 OES, United Kingdom

Although the cellular prion protein (PrP^C) is concentrated at synapses, the factors that target PrP^C to synapses are not understood. Here we demonstrate that exogenous PrP^C was rapidly targeted to synapses in recipient neurons derived from Prnp knock-out$^{(0/0)}$ mice. The targeting of PrP^C to synapses was dependent upon both neuronal cholesterol concentrations and the lipid and glycan composition of its glycosylphosphatidylinositol (GPI) anchor. Thus, the removal of either an acyl chain or sialic acid from the GPI anchor reduced the targeting of PrP^C to synapses. Isolated GPIs (derived from PrP^C) were also targeted to synapses, as was IgG conjugated to these GPIs. The removal of sialic acid from GPIs prevented the targeting of either the isolated GPIs or the IgG-GPI conjugate to synapses. Competition studies showed that pretreatment with sialylated GPIs prevented the targeting of PrP^C to synapses. These results are consistent with the hypothesis that the sialylated GPI anchor attached to PrP^C acts as a synapse homing signal.

The cellular prion protein (PrP^C)[2] gained prominence when it was identified as the normal isoform of the disease-associated protein (PrP^{Sc}) that accumulates in the brains of humans and animals with transmissible spongiform encephalopathies (1). That observation increased interest in the role of PrP^C in neurons. Reports that PrP^C is concentrated at synapses (2, 3) and that transgenic mice in which the gene for PrP had been knocked-out ($Prnp^{(0/0)}$) showed synaptic and memory deficits (4, 5) suggest that it plays a role in neurotransmission. The targeting of proteins to specific cellular locations may be critical for their function. For example, the proteins involved in synaptic vesicle recycling need to be delivered to the synapse in neurons. Little is known about the molecular mechanism(s) by which PrP^C accumulates within synapses. PrP^C is linked to cell membranes by a glycosylphosphatidylinositol (GPI) anchor (6), which affects the cellular distribution and function of PrP^C (7–9). PrP^C is found within cholesterol-rich, membrane microdomains that are commonly called lipid rafts (10, 11). Because only a small proportion of proteins that are found within lipid rafts are subsequently transported to synapses, the factors affecting the targeting of PrP^C to synapses were studied.

The GPI anchor that links PrP^C to the cell membrane targets it to lipid rafts (7). There are many different lipid rafts that demonstrate heterogeneity in their protein, glycolipid, and lipid composition (12), and different GPI-anchored proteins are targeted to different lipid rafts. For example, Thy-1 and PrP^C occupy separate domains on the neuronal surface (13). Although all GPI anchors contain a conserved core, variations on this core structure are common (14), and the GPI attached to PrP^C differs from that of Thy-1 (15, 16). It has been hypothesized that the localization of some GPI-anchored proteins to specific lipid rafts and hence specific cell membranes is due to the composition of the GPI anchor. Thus, the composition of GPI anchors directs antigens to different rafts in the absence of interactive external domains (17, 18), and the chemical composition of the GPI anchor alters the intracellular trafficking of proteins (19). Many GPI-anchored molecules are rapidly incorporated into living cells (20, 21). In this study, PrP^C was transferred to recipient cortical neurons derived from Prnp knock-out$^{(0/0)}$ mice. We demonstrate that the targeting of PrP^C to synapses was dependent upon cholesterol concentrations in the recipient neurons. Critically, we also demonstrate that the composition of the GPI anchor attached to PrP^C is a key factor that affects the targeting of PrP^C to synapses. More specifically, we show that the presence of sialic acid on the GPI anchor is necessary for the targeting of PrP^C to synapses.

Results

PrP^C Is Targeted to Synapses—To study the factors that control the targeting of PrP^C to synapses, PrP^C (10 nM) was introduced into neurons derived from $Prnp^{(0/0)}$ mice (22). PrP^C preparations run in gels and stained with Coomassie Brilliant Blue did not show any contaminants (Fig. 1*A*). After 2 h, recipient neurons were collected, and organelles were separated upon a Percoll density gradient. The synaptic protein synaptophysin, used to identify synaptosomes, was concentrated in fractions 42–46 (Fig. 1*B*). These fractions also contained high concentrations of the synaptic proteins synapsin-1 and synaptobrevin-1 and were consequently pooled as synaptosomes. Following introduction to neurons, PrP^C showed a time-dependent (Fig. 1*C*) and concentration-dependent (Fig. 1*D*) accumulation within synaptosomes. Not all GPI-anchored proteins were targeted to synapses because GPI-anchored CD14 added to neurons did not accumulate within synapses.

* This work was supported by the European Commission FP6 "Neuroprion," Network of Excellence. The authors declare that they have no conflicts of interest with the contents of this article.
[1] To whom correspondence should be addressed. Tel.: 44-1223-337640; Fax: 44-1223-335908; E-mail: aw510@cam.ac.uk.
[2] The abbreviations used are: PrP^C, cellular prion protein; GPI, glycosylphosphatidylinositol; DRM, detergent-resistant membrane; DSM, detergent-sensitive membrane; HPTLC, high performance thin layer chromatography; PI-PLC, phosphatidylinositol-specific phospholipase C; CSP, cysteine string protein.

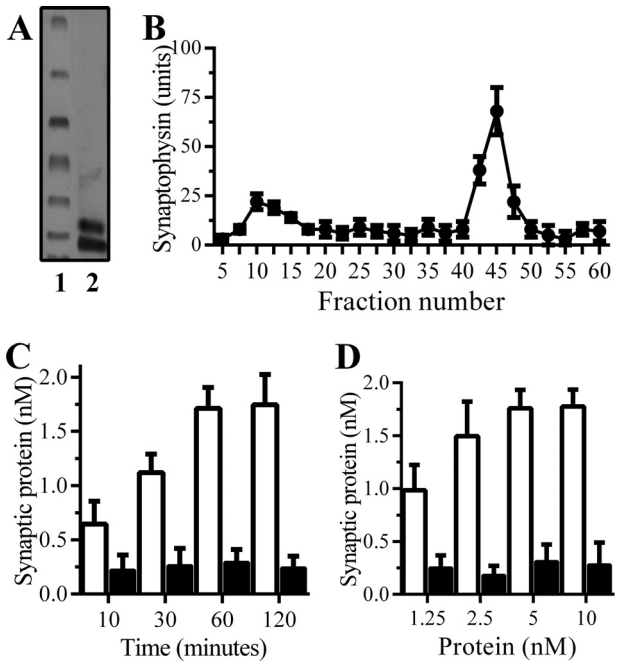

FIGURE 1. **PrP^C is targeted to the synapses.** *A*, Coomassie Brilliant Blue-stained gel showing protein ladder (*lane 1*) and neuronal PrP^C (*lane 2*). *B*, amounts of synaptophysin in fractions derived from Prnp$^{(0/0)}$ neurons separated on a Percoll density gradient. Values are means ± S.D. (*error bars*) from an experiment measured in quadruplicate. *C*, concentrations of PrP^C (□) or CD14 (■) in synaptosomes derived from Prnp$^{(0/0)}$ neurons incubated with 10 nM proteins for time periods as shown. Values are means ± S.D. from duplicate experiments performed five times ($n = 10$). *D*, concentrations of PrP^C (□) or CD14 (■) in synaptosomes from Prnp$^{(0/0)}$ neurons incubated with proteins as shown for 2 h. Values are means ± S.D. from duplicate experiments performed five times ($n = 10$).

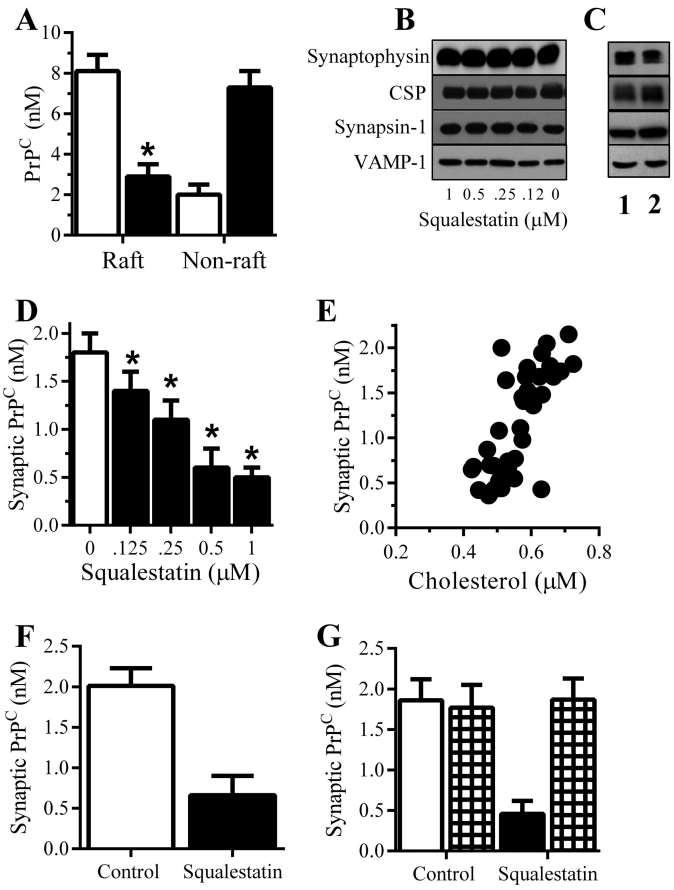

FIGURE 2. **Cholesterol depletion reduced the targeting of PrP^C to synapses.** *A*, concentrations of PrP^C in raft and non-raft membranes from Prnp$^{(0/0)}$ neurons pretreated with a vehicle control (□) or 1 μM squalestatin (■) and incubated with 10 nM PrP^C for 2 h. Values are means ± S.D. (*error bars*) from triplicate experiments performed four times ($n = 12$). *, raft PrP^C significantly less than in control neurons. *B*, immunoblots showing the amounts of synaptophysin, CSP, synapsin-1, and VAMP-1 in neurons incubated with squalestatin as shown. *C*, immunoblotting showing the amounts of synaptic proteins in synaptosomes treated with control medium (*lane 1*) or 1 μM squalestatin (*lane 2*). *D*, concentrations of PrP^C in synaptosomes from Prnp$^{(0/0)}$ neurons pretreated with a vehicle control (□) or squalestatin as shown (■) and incubated with 10 nM PrP^C for 2 h. Values are means ± S.D. from triplicate experiments performed four times ($n = 12$). *, synaptic PrP^C significantly less than in control neurons. *E*, there was a significant correlation between cholesterol concentrations in Prnp$^{(0/0)}$ neurons treated with squalestatin (range from 1 μM to 125 nM) and the concentrations of PrP^C in synaptosomes following incubation with 10 nM PrP^C for 2 h (Pearson's coefficient = 0.73, $p < 0.01$). *F*, concentrations of PrP^C in synaptosomes from Prnp$^{(+/+)}$ neurons treated with a vehicle control (□) or 1 μM squalestatin (■) for 2 h. Values are means ± S.D. from triplicate experiments performed three times ($n = 9$). *G*, concentrations of PrP^C in synaptosomes from Prnp$^{(0/0)}$ neurons pretreated with a vehicle control or 1 μM squalestatin as shown (■) mixed with 5 μM squalene (*checkered bars*) and incubated with 10 nM PrP^C for 2 h. Values are means ± S.D. from triplicate experiments performed three times ($n = 9$).

Targeting of PrP^C to Synapses Is Sensitive to Cholesterol Depletion—PrP^C is found in lipid rafts that contain high concentrations of cholesterol (11). Because cholesterol depletion affects the expression of PrP^C (7, 23, 24), the effects of cholesterol depletion on the targeting of PrP^C to synapses were examined. Prnp$^{(0/0)}$ neurons were treated with squalestatin, a selective squalene synthase inhibitor that reduced neuronal cholesterol concentrations (25). Although treatment with 1 μM squalestatin did not affect the uptake of exogenous PrP^C into neurons (9.3 nM PrP^C ± 0.6 compared with 9.2 nM ± 0.5, $n = 9$, $p = 0.68$), it significantly reduced the concentrations of PrP^C found in lipid rafts (detergent-resistant membranes (DRMs)) (Fig. 2*A*). Although cholesterol is required for the formation and maintenance of synapses (26, 27), the mild cholesterol depletion caused by 1 μM squalestatin did not significantly alter the concentrations of synaptophysin, cysteine string protein (CSP), synapsin-1, or VAMP-1 (vesicle-associated membrane protein 1) in neurons (Fig. 2*B*) or isolated synaptosomes (Fig. 2*C*), indicating that it did not damage synapses. When Prnp$^{(0/0)}$ neurons were treated with squalestatin for 24 h and incubated with 10 nM PrP^C, squalestatin caused a dose-dependent reduction in the concentrations of PrP^C found within synaptosomes (Fig. 2*D*). There was a significant correlation between cholesterol concentrations in squalestatin-treated neurons and the concentrations of PrP^C found in synapses (Pearson's coefficient = 0.73, $p < 0.01$) (Fig. 2*E*). Treatment of Prnp$^{(+/+)}$ wild-type neurons with 500 nM squalestatin reduced the concentrations of PrP^C in synaptosomes (Fig. 2). The addition of 5 μM squalene reversed the effects of squalestatin upon neuronal cholesterol concentrations (23) and PrP^C trafficking to synapses (Fig. 2*G*).

Monoacylated PrP^C Is Not Targeted to Synapses—PrP^C was digested with PLA_2, an enzyme that targets acyl chains contained within GPIs to form monoacylated PrP^C (Fig. 3*B*) and isolated using an immunoaffinity column and reverse phase chromatography as described (8). Although similar amounts of monoacylated PrP^C and PrP^C bound to recipient Prnp$^{(0/0)}$ neurons (9.4 nM PrP^C ± 0.7 compared with 9.2 nM ± 0.5, $n = 12$,

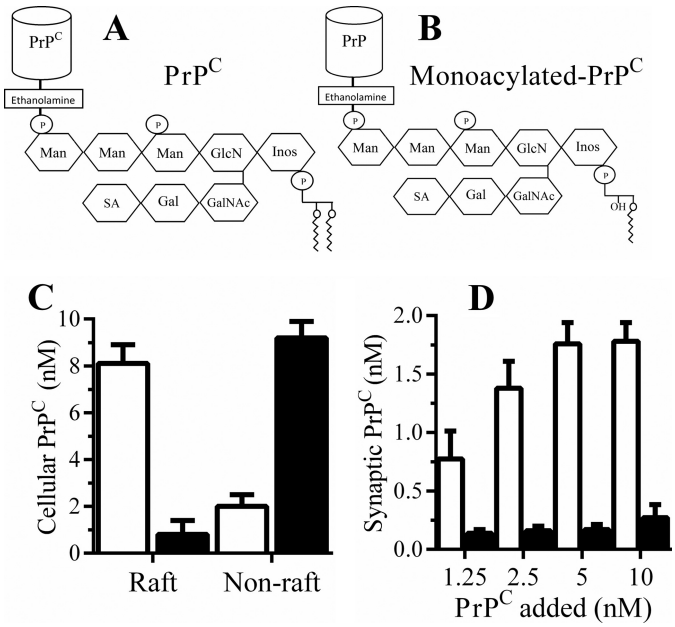

FIGURE 3. **Monoacylated PrP^C is not targeted to synapses.** Schematics show the putative structure of the GPIs attached to PrP^C (*A*) and monoacylated PrP^C (*B*). Glycan residues shown include mannose (*Man*), sialic acid (*SA*), galactose (*Gal*), *N*-acetyl galactosamine (*GalNAc*), inositol (*Inos*), and glucosamine (*GlcN*). *C*, concentrations of PrP^C (□) and monoacylated PrP^C (■) in raft and non-raft membranes derived from Prnp$^{(0/0)}$ neurons incubated with 10 nM PrP^C/monoacylated PrP^C for 2 h. Values are means ± S.D. (*error bars*) from triplicate experiments performed three times ($n = 9$). *D*, the concentrations of PrP^C in synaptosomes derived from Prnp$^{(0/0)}$ neurons incubated with PrP^C (□) or monoacylated PrP^C (■) as shown for 2 h. Values are means ± S.D. from duplicate experiments performed five times ($n = 10$).

$p = 0.3$), they were differently distributed between membranes. Whereas the majority of PrP^C was found within lipid rafts (DRMs), most of the monoacylated PrP^C was found within detergent-soluble membranes (DSMs) (Fig. 3*C*). Monoacylated PrP^C added to Prnp$^{(0/0)}$ neurons was not targeted to synaptosomes (Fig. 3*D*).

Glia-derived PrP^C Did Not Target Synapses—Because PrP^C is also expressed by glial cells, we sought to determine whether glia-derived and neuron-derived PrP^C had the same properties. Prnp$^{(0/0)}$ neurons were incubated with 10 nM glia-derived PrP^C or 10 nM neuron-derived PrP^C for 2 h. There were no significant differences in the concentrations of glial and neuronal PrP^C incorporated into recipient neurons; nor were there any significant differences in the concentrations found within DRMs (Table 1). However, glial PrP^C did not accumulate within synaptosomes (Fig. 4*A*). By comparing neuron and glia-derived PrP^C we sought to determine the factors that affect synaptic targeting. Because the glycosylation of PrP^C affects the trafficking of PrP^C (28, 29), the possibility that cell-specific glycosylation affected the targeting of PrP^C to synapses was examined. PNGase removed the *N*-linked glycans from PrP^C (30). When Prnp$^{(0/0)}$ neurons were pulsed with 10 nM neuronal PrP^C or 10 nM PNGase-digested neuronal PrP^C for 2 h, we found that the removal of *N*-linked glycans did not alter the concentrations of PrP^C that bound to recipient neurons or the concentrations of PrP^C found within synaptosomes (Table 1 and Fig. 4*B*). PNGase-digested glial PrP^C was not found within synaptosomes, indicating that *N*-linked glycans did not stop glial PrP^C from targeting synapses (Table 1). To eliminate the possible

TABLE 1

***N*-linked glycans do not affect the targeting of PrP^C to synapses**

The concentrations of PrP^C in cell extracts, DRMs, DSMs, and synaptosomes isolated from Prnp$^{(0/0)}$ neurons were incubated with 10 nM neuron-derived PrP^C, 10 nM PNGase-digested neuron-derived PrP^C, 10 nM glia-derived PrP^C, or 10 nM PNGase-digested glia-derived PrP^C for 2 h. Values are means ± S.D. from triplicate experiments performed four times ($n = 12$).

	Concentration PrP^C			
	Total	DRM	DSM	Synapse
			nM	
Neuronal PrP^C	9.2 ± 0.9	8.5 ± 0.8	1.0 ± 0.4	1.8 ± 0.32
PNGase-digested neuronal PrP^C	8.9 ± 0.6	8.2 ± 0.8	0.9 ± 0.3	1.9 ± 0.35
Glial PrP^C	9.2 ± 1.0	8.6 ± 0.8	1.1 ± 0.3	0.29 ± 0.24[a]
PNGase-digested glial PrP^C	9.0 ± 0.5	8.0 ± 0.9	1.1 ± 0.4	0.24 ± 0.18[a]

[a] Concentration of PrP^C in synaptosomes significantly less than in neurons incubated with neuron-derived PrP^C.

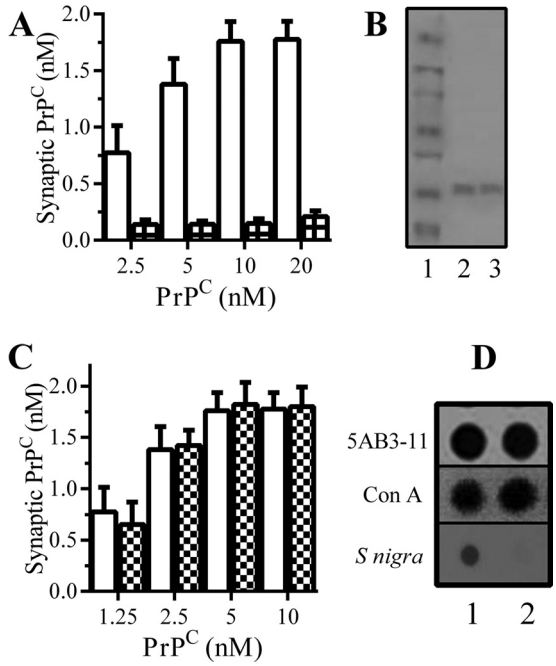

FIGURE 4. **Glia-derived PrP^C is not targeted to synapses.** *A*, concentrations of PrP^C in synaptosomes from Prnp$^{(0/0)}$ neurons incubated for 2 h with neuronal PrP^C (□) or glial PrP^C (*hatched bars*) as shown. Values are means ± S.D. (*error bars*) from triplicate experiments performed three times ($n = 9$). *B*, Coomassie Brilliant Blue-stained gel showing protein ladder (*lane 1*), deglycosylated glial PrP^C (*lane 2*), and deglycosylated neuronal PrP^C (*lane 3*). *C*, concentrations of PrP^C in synaptosomes from Prnp$^{(0/0)}$ neurons incubated for 2 h with neuronal PrP^C (□) or endoglycosidase F-digested neuronal PrP^C (*checkered bars*) as shown. Values are means ± S.D. from duplicate experiments performed five times ($n = 10$). *D*, dot blots showing the binding of mAb 5AB3-11 (phosphatidylinositol), concanavalin A (mannose), or *S. nigra* lectin (sialic acid) to GPIs isolated from neuronal PrP^C (*lane 1*) or glial PrP^C (*lane 2*).

effects of *N*-linked glycans on the trafficking of PrP^C, all subsequent experiments were carried out on PNGase-digested PrP^C preparations.

Because the composition of the GPI anchor is dependent upon the cell type (31, 32), the nature of GPIs attached to glial and neuronal PrP^C was determined. Isolated GPIs from neuronal and glial PrP^C were blotted onto nitrocellulose membranes. Detection with the phosphatidylinositol-reactive mAb 5AB3-11 and biotinylated concanavalin A (which binds to mannose, a core component of all GPIs) showed that similar amounts of GPIs were loaded onto membranes. However, *Sambucus nigra* lectin (which reacts with terminal sialic acid bound either α-2,6 or α-2,3 to galactose) bound to GPIs isolated from

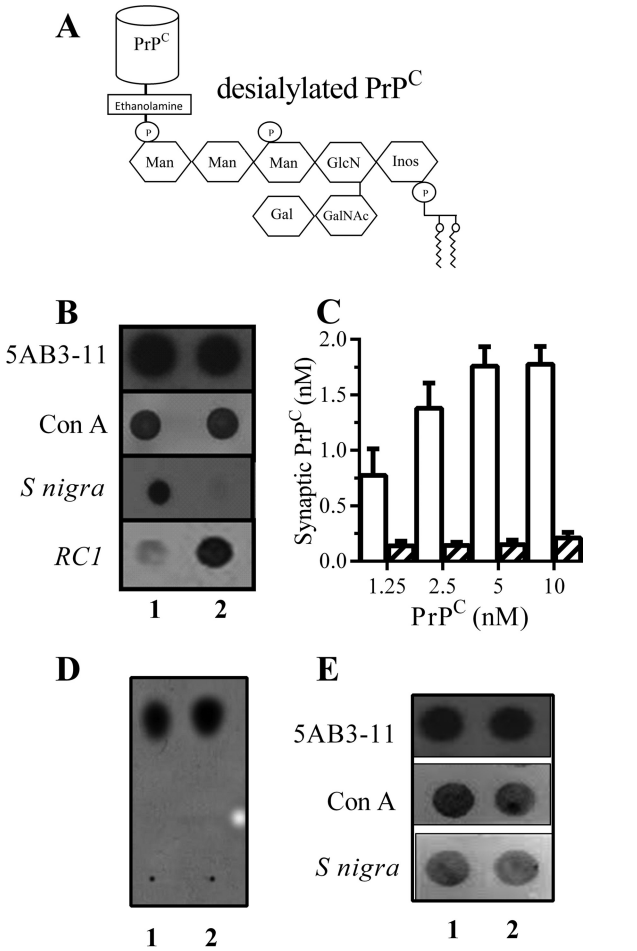

FIGURE 5. **Desialylated PrP^C is not targeted to synapses.** *A*, putative structure of the GPI attached to neuronal PrP^C after digestion with neuraminidase. *B*, dot blots showing the binding of mAb 5AB3-11 (phosphatidylinositol), concanavalin A (mannose), *S. nigra* lectin (sialic acid), or RC1 (galactose) to GPIs isolated from PrP^C (*lane 1*) and desialylated PrP^C (*lane 2*). *C*, concentrations of PrP^C in synaptosomes from Prnp$^{(0/0)}$ neurons incubated for 2 h with PrP^C (□) or desialylated PrP^C (*striped bars*) as shown. Values are means ± S.D. (*error bars*) from triplicate experiments performed three times ($n = 9$). *D*, GPIs derived from neuronal PrP^C isolated from synaptosomes (*lane 1*) or from the cell body (*lane 2*) separated by HPTLC. *E*, dot blots showing the binding of mAb 5AB3-11 (phosphatidylinositol), concanavalin A (mannose), or *S. nigra* lectin (terminal sialic acid) to GPIs attached to PrP^C isolated from synaptosomes (*lane 1*) or from the neuronal cell body (*lane 2*).

neuronal PrP^C but not glial PrP^C (Fig. 4*C*), indicating that only the GPI attached to neuronal PrP^C contained a terminal sialic acid.

Desialylated PrP^C Does Not Target Synapses—The composition of GPI anchors affects the targeting of proteins to specific membranes (20, 33). This sialic acid on GPIs derived from neuronal PrP^C is susceptible to neuraminidase digestion (34), resulting in desialylated PrP^C (Fig. 5*A*). Digestion of neuronal PrP^C with neuraminidase reduced the binding of *S. nigra* lectin without affecting the binding of concanavalin A or the phosphatidylinositol-reactive mAb 5AB3-11. Neuraminidase removal of terminal sialic acid would be expected to reveal a galactose residue (Fig. 5*A*). The lectin RC1 (which reacts with terminal galactose) binds to GPIs derived from desialylated PrP^C but not to GPIs from neuronal PrP^C, consistent with the putative structure of PrP^C GPIs as proposed by Stahl *et al.* (15) (Fig. 5*B*). Similar amounts of PrP^C and desialylated PrP^C bound to Prnp$^{(0/0)}$ neurons and were found within DRMs (Table 1). Although both neuronal and desialylated PrP^C were targeted to rafts, desialylated PrP^C did not accumulate in synapses (Fig. 5*C*).

To determine whether the GPI attached to PrP^C found at synapses differed from that found in the cell body, synaptosomes from Prnp$^{(+/+)}$ wild-type neurons were isolated. PrP^C was purified, and GPIs were isolated. There were no obvious differences between GPIs isolated from synaptic PrP^C or from cell body PrP^C when analyzed by high performance thin layer chromatography (HPTLC) (Fig. 5*D*) or by dot blots (Fig. 5*E*). The *S. nigra* lectin (which binds terminal sialic acid) bound to GPIs isolated from PrP^C derived from the cell body.

Isolated GPIs Are Targeted to Synapses—GPIs from neuronal PrP^C and desialylated PrP^C were isolated on C18 columns (Fig. 6*A*) and HPTLC (Fig. 6*B*) and labeled with FITC. Prnp$^{(0/0)}$ neurons were incubated with 10 nM FITC or 10 nM FITC-labeled GPIs for 2 h and washed, and florescence was measured. Neurons incubated with 10 nM FITC contained only 0.6 nM ± 0.2 FITC compared with neurons incubated with FITC-GPI (8.2 nM ± 0.88) or FITC-desialylated GPI (7.7 nM ± 0.98) (Table 2). Similar concentrations of GPIs and desialylated GPIs were found in lipid rafts (DRMs) (Table 2). GPIs derived from neuronal PrP^C accumulated in synaptosomes in a dose-dependent manner (Fig. 6*C*). FITC-GPIs accumulated in synaptosomes at higher concentrations than FITC alone or desialylated GPIs (Fig. 6*D*).

To determine whether GPIs inhibited the targeting of neuronal PrP^C to synaptosomes, Prnp$^{(0/0)}$ neurons were pretreated with GPIs derived from PrP^C (10 to 1.25 nM) and incubated with 10 nM neuronal PrP^C for 2 h. These GPIs reduced the concentrations of PrP^C found within synaptosomes in a dose-dependent manner (Fig. 6*E*). This effect was structure-dependent because desialylated GPIs did not affect the concentrations of PrP^C found within synaptosomes (Fig. 6*F*).

GPIs Target IgG to Synapses—To test the hypothesis that specific GPIs could target other proteins to synapses, rabbit IgG was conjugated to GPIs (derived from neuronal PrP^C) or desialylated GPIs. The GPI-modified rabbit IgG was isolated by reverse phase chromatography on C18 columns. IgG conjugated to GPIs or desialylated GPIs eluted from C18 columns in concentrations between 60 and 70%, whereas control IgG did not bind and eluted in the void volume (Fig. 7*A*). IgG conjugated to GPIs was differentiated from IgG by HPTLC (Fig. 7*B*). Subsequently, neurons were incubated with 10 nM IgG, 10 nM IgG-GPI, or 10 nM IgG-desialylated GPI for 2 h. Only low concentrations of IgG (0.3 nM) bound to neurons. Similar concentrations of IgG-GPI and IgG-desialylated GPI were found in neurons, indicating that the composition of the GPI did not affect the binding to neurons (Fig. 7*C*). Both IgG-GPI and IgG-desialylated GPI were targeted to lipid rafts (DRMs) (Table 3). Both were released from neurons by digestion with phosphatidylinositol-specific phospholipase C (PI-PLC), indicating that they were expressed at the surface of neurons (Table 3). Critically, IgG-GPI, but not IgG-desialylated GPI, was found in synaptosomes (Fig. 7*D*).

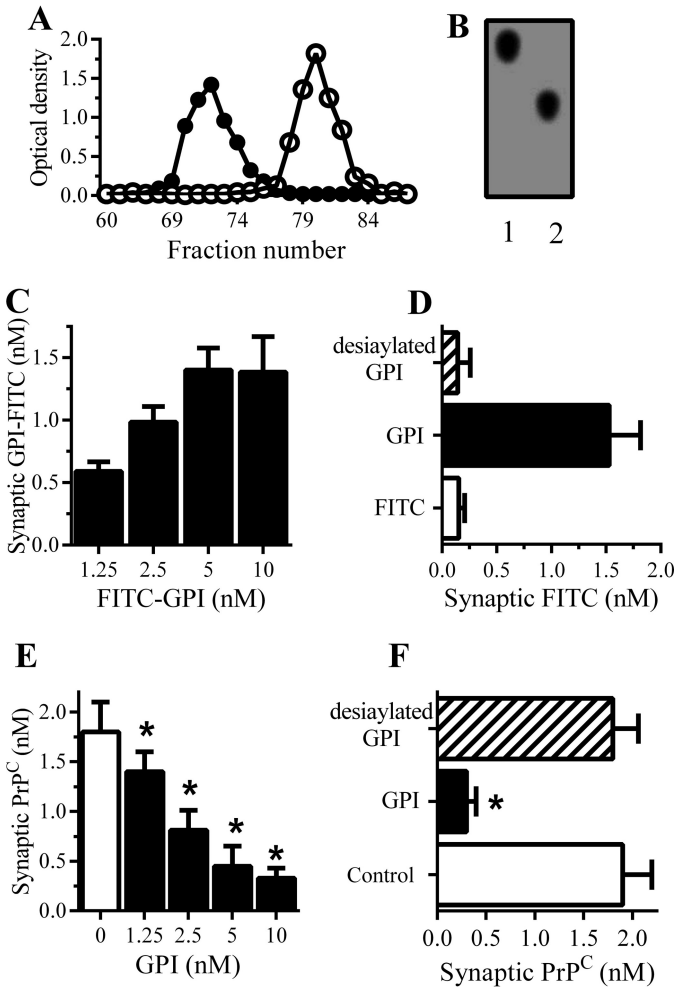

FIGURE 6. **Desialylated GPIs do not target synapses.** *A*, GPIs derived from neuronal PrP^C (○) and desialylated GPIs (●) eluted from C18 columns. Values are means of duplicates. *B*, GPIs derived from neuronal PrP^C (*lane 1*) and desialylated GPIs (*lane 2*) separated by HPTLC. *C*, amounts of FITC in synaptosomes from neurons incubated for 2 h with FITC-labeled GPIs as shown. Values are means ± S.D. (*error bars*) from triplicate experiments performed twice ($n = 6$). *D*, amounts of FITC in synaptosomes from neurons incubated for 2 h with 10 nM FITC alone (□) or with 10 nM FITC-labeled GPIs (■) or 10 nM FITC-desialylated GPIs (*striped bar*). Values are means ± S.D. from triplicate experiments performed twice ($n = 6$). *E*, concentrations of PrP^C in synaptosomes isolated from $Prnp^{(0/0)}$ neurons pretreated with control medium (□) or GPIs as shown (■) and incubated with 10 nM PrP^C. Values are means ± S.D. from triplicate experiments performed two times ($n = 6$). *, significantly less synaptic PrP^C than in control synaptosomes. *F*, concentrations of PrP^C in synaptosomes isolated from $Prnp^{(0/0)}$ neurons pretreated with control medium (□), 10 nM GPIs (■), or 10 nM desialylated GPIs (*striped bar*) and incubated with 10 nM PrP^C. Values are means ± S.D. from triplicate experiments performed two times ($n = 6$). *, significantly less synaptic PrP^C than in control synaptosomes.

TABLE 2
GPIs are targeted to rafts

Shown are the concentrations of GPIs in $Prnp^{(0/0)}$ neurons incubated with 10 nM FITC (as a control) or 10 nM FITC conjugated to GPI or desialylated GPI for 2 h when cell extracts, DRMs, and DSMs were isolated. Values are means ± S.D. from triplicate experiments performed 4 times ($n = 12$).

	FITC (Fluorescence)		
	Total	DRM	DSM
		nM	
FITC-control	0.6 ± 0.2	0.2 ± 0.2	0.4 ± 0.2
FITC-GPI	8.2 ± 0.88	7.6 ± 0.64[a]	0.53 ± 0.21
FITC-desialylated GPI	7.7 ± 0.98	7.2 ± 0.71[a]	0.51 ± 0.25

[a] Concentration of GPIs in DRMs (rafts) significantly less than in neurons incubated with control GPIs.

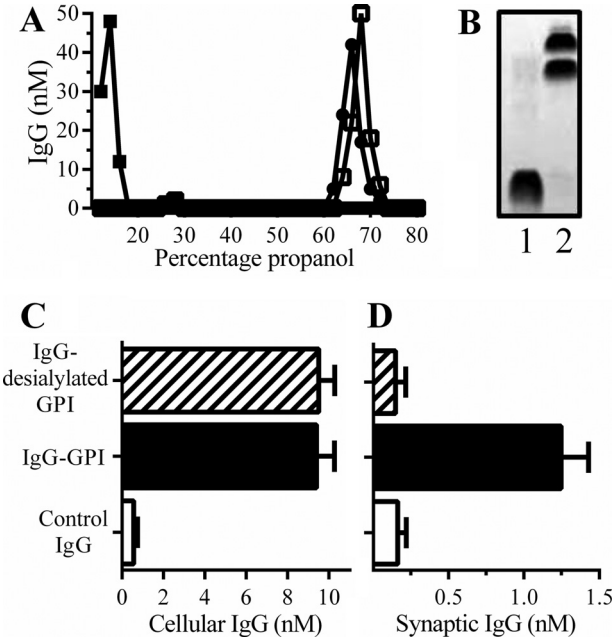

FIGURE 7. **Sialylated GPIs targeted IgG to synapses.** *A*, concentrations of IgG (■), IgG-GPI (●), or IgG-desialylated GPI (□) in fractions eluted off of C18 columns under a gradient of propanol and water. *B*, IgG (*lane 1*) and IgG-GPI (*lane 2*) separated by HPTLC. *C*, concentrations of IgG in neurons incubated with 10 nM IgG (□), 10 nM IgG-GPI (■), or 10 nM IgG-desialylated GPI (*striped bar*) for 2 h. Values are means ± S.D. (*error bars*) from triplicate experiments performed three times ($n = 9$). *D*, concentrations of IgG in synaptosomes derived from neurons incubated with 10 nM IgG (□), 10 nM IgG-GPI (■), or 10 nM IgG-desialylated GPI (*striped bar*) for 2 h. Values are means ± S.D. from triplicate experiments performed three times ($n = 9$).

Discussion

Our study examined the factors that affect the distribution of PrP^C in neurons. We report that PrP^C added to recipient $Prnp^{(0/0)}$ neurons rapidly accumulated at synapses. The targeting of PrP^C to synapses was dependent upon two key factors: the cholesterol concentration of cell membranes and the composition of the GPI attached to PrP^C. More specifically, PrP^C was not targeted to synapses following the removal of either sialic acid or an acyl chain from the GPI attached to PrP^C.

The targeting of proteins to specific membrane domains is of key importance in neurons. PrP^C is concentrated in synapses (2, 3), and in this study, neuron-derived PrP^C was targeted to synapses after its inclusion in specific, cholesterol-sensitive, lipid rafts. The mild cholesterol depletion caused by squalestatin did not affect the number of synapses. However, this cholesterol depletion reduced the targeting of neuronal PrP^C to lipid rafts and the trafficking of PrP^C to synapses (there was a significant correlation between the concentrations of cholesterol in squalestatin-treated neurons and the concentrations of PrP^C found within synaptosomes), results consistent with the hypothesis that the inclusion of PrP^C into lipid rafts precedes delivery of PrP^C to synapses. Squalestatin also reduced the concentrations of PrP^C found in synaptosomes from wild type neurons. The effect of squalestatin on cholesterol concentrations and the targeting of PrP^C to rafts and synaptosomes were reversed by the addition of squalene.

We hypothesized that the GPI also targeted PrP^C to synapses. This hypothesis was supported by the observation that monoacylated PrP^C was neither targeted to rafts nor found in syn-

TABLE 3

Sialylated GPIs target IgG to rafts

Shown are the concentrations of rabbit IgG in neurons incubated with 10 nM rabbit IgG (as a control), 10 nM rabbit IgG-GPI, or 10 nM IgG-desialylated GPI for 2 h when cell extracts, DRMs, and DSMs were collected. Also shown are the concentrations of IgG in neurons following digestion with PI-PLC. Values are means ± S.D. from triplicate experiments performed four times ($n = 12$).

	Rabbit IgG			
	Total	DRM	DSM	PI-PLC
	nM			
Control IgG	0.3 ± 0.1	0.1 ± 0.1	0.1 ± 0.1	0.1 ± 0.1
IgG-GPI	9.1 ± 0.4	8.4 ± 0.5	0.8 ± 0.2	0.2 ± 0.2
IgG-desialylated GPI	9.2 ± 0.5	8.5 ± 0.7	0.8 ± 0.2	0.1 ± 0.1

apses. It is thought that saturated acyl chains attached to GPIs allow tight molecular packing and increase the solubilization of cholesterol (35, 36). Consequently, the loss of a saturated acyl chain disrupts the membrane surrounding monoacylated PrP^C (8). Not all GPI-anchored proteins found within rafts are found within synapses, and neither the GPI-anchored CD14 nor glial PrP^C was found within synaptosomes. The observation that glial PrP^C was not found within synapses indicated that the essential synaptic targeting signal in PrP^C lay in a post-translational modification. Because digestion with PNGase did not affect the trafficking of PrP^C to synapses, we concluded that *N*-linked glycosylation of neuronal and glial PrP^C was not a significant factor in targeting PrP^C to synapses.

The composition of the GPI anchor is dependent upon the cell type (31, 32), and the structure of the GPI attached to PrP^C can vary (15). Whereas the GPI attached to neuronal PrP^C contains sialic acid, GPIs derived from glial PrP^C did not, suggesting that the presence of sialic acid on the GPI attached to neuronal PrP^C was a key factor that targeted it to synapses. This hypothesis was supported by observations that the removal of sialic acid from neuronal PrP^C reduced its migration to synapses. Notably, desialylated neuronal PrP^C and glial PrP^C had similar properties; both targeted lipid rafts and were predominantly expressed at the surface of recipient neurons. The composition of GPI targets proteins to different lipid rafts (17, 33, 37) that traffic via different pathways (9, 19), indicating how the composition of the GPI can affect the trafficking of PrP^C. Thus, whereas PrP^C with a sialylated GPI enters a pathway that ends at the synapse, desialylated PrP^C targeted a different raft and trafficked to a different cellular location.

GPI-anchored proteins are surrounded by lipid shells that are dependent on multiple protein-lipid, glycan-lipid, and lipid-lipid interactions (38). The concept that the molecular structure of the GPI may regulate the composition of the underlying membrane was supported by observations that Thy-1 and PrP^C have different GPI anchors (15, 16) and occupy separate domains on the neuronal surface (13), which have different lipid compositions (40). Similarly, desialylated PrP^C is associated with membrane rafts containing greater concentrations of gangliosides and cholesterol than native PrP^C (41). It is noteworthy that gangliosides help sequester cholesterol and stabilize rafts (42–44) and affect the distribution and trafficking of GPI-anchored proteins (45, 46), including PrP^C (47). The increased association of desialylated PrP^C with gangliosides helps explain why desialylated PrP^C showed greater resistance to cholesterol depletion than did neuronal PrP^C.

These results suggested that the synapse-targeting information is contained within the GPI alone, which is consistent with reports that the glycan composition of GPIs direct antigens to specific membrane microdomains in the absence of interactive external domains (18, 33). The targeting of isolated GPIs (derived from PrP^C) also required the presence of sialic acid. The role of the GPI as a major "synapse-targeting" signal was demonstrated when isolated GPIs were conjugated to rabbit IgG. IgG was not readily taken up by neurons and was not found within synapses. In contrast, IgG conjugated to GPIs derived from neuronal PrP^C inserted into recipient neurons and was targeted to synapses. Although IgG conjugated to desialylated GPIs also inserted into neurons, it was not found within synapses. Such results suggest a novel mechanism of cell engineering whereby proteins could be targeted to synapses by the attachment of specific GPIs.

The maximum concentration of PrP^C measured in synapses of recipient neurons, regardless of how much PrP^C was added, was ~2 nM. Similar concentrations of PrP^C were found in synaptosomes from Prnp wild-type neurons, suggesting that the process by which PrP^C traffics to synapses is limited. In a similar manner, the concentrations of isolated GPIs found at synapses were also limited. The observation that pretreatment with isolated GPIs reduced the targeting of neuronal PrP^C to synapses supported the hypothesis that PrP^C and isolated GPIs compete for the same synapse-targeting pathways. This hypothesis is supported by the observation that the capacity of GPIs to block the targeting of neuronal PrP^C to synapses was also dependent upon the presence of sialic acid.

In conclusion, we demonstrated the role of GPIs as targeting signals in neurons. The targeting of PrP^C to synapses was dependent upon the structure of the GPI anchor requiring the presence of two acyl chains and sialic acid. The composition of the GPI anchor alone contained sufficient information to target synapses in the absence of the external protein domain.

Experimental Procedures

Primary Neuronal Cultures—Cortical neurons were prepared from the brains of mouse embryos (day 15.5) from both Prnp wild-type$^{(+/+)}$ and Prnp knock-out$^{(0/0)}$ mice. Neurons were plated at 1×10^6 cells/well in 6-well plates (precoated with poly-L-lysine) in Ham's F-12 containing 5% fetal calf serum for 2 h. Cultures were then shaken (600 rpm for 5 min), and non-adherent cells were removed by three washes in PBS. Neurons were grown in neurobasal medium containing B27 components and nerve growth factor (5 ng/ml) (Sigma) for 10 days. Immunohistochemistry showed that the cells were greater than 95% neurofilament-positive. For cell-targeting studies, neurons were incubated with PrP^C preparations for different time periods. In some experiments, neurons were pretreated with test compounds (drugs, PrP preparations, and isolated GPIs) and incubated with test preparations.

Cell Extracts—Neurons were homogenized in an extraction buffer containing 150 mM NaCl, 10 mM Tris-HCl, pH 7.4, 10 mM EDTA, 0.5% Nonidet P-40, 0.5% sodium deoxycholate, 0.2% SDS, and mixed protease inhibitors (4-(2-aminoethyl) benzenesulfonyl fluoride hydrochloride, aprotinin, leupeptin, bestatin, pepstatin A, and E-46) (Sigma) and a phosphatase

inhibitor mixture including PP1, PP2A, microcystin LR, cantharidin, and *p*-bromotetramisole (Sigma) at 10^6 cells/ml. Nuclei and cell debris were removed by centrifugation (500 × *g* for 5 min).

Isolation of Synaptosomes—Synaptosomes were prepared on a discontinuous Percoll gradient as described (48). Briefly, neurons were homogenized at 4 °C in 1 ml of SED solution (0.32 M sucrose, 5 mM Tris-HCl, pH 7.2, 1 mM EDTA, and 0.25 mM dithiothreitol) and centrifuged at 1000 × *g* at 4 °C. The supernatant was transferred to a four-step gradient of 3, 7, 15, and 23% Percoll in SED solution and centrifuged at 16,000 × *g* for 30 min at 4 °C. The synaptosomes were collected from the interface between the 15 and 23% Percoll and washed (16,000 × *g* for 10 min at 4 °C) and suspended in neurobasal medium containing B27 components. All synaptosomes were used on the same day of preparation; freshly prepared synaptosomes were incubated with peptides for 1 h. After the test period, synaptosomes were homogenized in either extraction buffer (as above) or in the DRM extraction buffer (as below). All synaptosome preparations contained equal amounts of synaptophysin.

Western Blotting—Samples were mixed with Laemmli buffer containing β-mercaptoethanol and heated to 95 °C for 5 min, and proteins were separated by electrophoresis on 15% polyacrylamide gels. Proteins were transferred onto a Hybond-P polyvinylidene fluoride membrane by semidry blotting. Membranes were blocked using 10% milk powder; synapsin-1 was detected with goat polyclonal antibody (Santa Cruz Biotechnology), synaptophysin with MAB368 (Abcam), CSP with rabbit polyclonal anti-CSP (sc-33154, Santa Cruz Biotechnology), VAMP-1 with mAb 4H302 (Abcam), caveolin with rabbit polyclonal antibodies to caveolin (Upstate), and PrP^C with mAb 4F2 (J. Grassi). These were visualized using a combination of biotinylated anti-mouse/goat/rat/rabbit IgG (Sigma), extravidin-peroxidase, and enhanced chemiluminescence.

Isolation of DRMs—These membranes were isolated by their insolubility in non-ionic detergents as described (49). Briefly, samples were homogenized in an ice-cold buffer containing 1% Triton X-100, 10 mM Tris-HCl, pH 7.2, 150 mM NaCl, 10 mM EDTA, and mixed protease and phosphatase inhibitors, and nuclei and large fragments were removed by centrifugation (300 × *g* for 5 min at 4 °C). The postnuclear supernatant was incubated on ice (4 °C) for 1 h with intermittent shaking and centrifuged (16,000 × *g* for 30 min at 4 °C). The supernatant was reserved as the DSM, whereas the pellet was homogenized in an extraction buffer (as above) and centrifuged (10 min at 16,000 × *g*), and the soluble material was reserved as the DRM fraction.

Synaptophysin ELISA—The amounts of synaptophysin in neurons were measured by ELISA (50). Maxisorb immunoplates were coated with 0.5 μg/ml mouse anti-synaptophysin mAb (MAB368, Chemicon, Darmstadt, Germany) and blocked with 5% milk powder. Samples were added for 1 h, and bound synaptophysin was detected with rabbit polyclonal anti-synaptophysin (Abcam) followed by biotinylated anti-rabbit IgG, extravidin-alkaline phosphatase, and 1 mg/ml 4-nitrophenol phosphate (Sigma). Absorbance was measured on a microplate reader at 405 nm. Samples were expressed as "units of synaptophysin," where 100 units was defined as the amount of synaptophysin in 10^6 control neurons.

Cholesterol—The concentrations of cholesterol in samples were measured using the Amplex Red cholesterol assay kit (Invitrogen) according to the manufacturer's instructions. Briefly, cholesterol was oxidized by cholesterol oxidase to yield hydrogen peroxide and ketones. The hydrogen peroxide reacted with 10-acetyl-3,7-dihydroxyphenoxazine (Amplex Red reagent) to produce highly fluorescent resorufin, which was measured by excitation at 550 nm and emission detection at 590 nm.

Isolation of PrP^C—PrP^C molecules were isolated from neurons or from N9 glial cells that had been homogenized in an extraction buffer (as above), and cell debris and nuclei were removed by centrifugation. The postnuclear supernatant was incubated with an affinity column loaded with mAb ICSM35 (M. Tayebi), and PrP^C was eluted using glycine-HCl at pH 2.7, neutralized with 1 M Tris, and desalted. These PrP^C preparations were further purified using size exclusion chromatography (Superdex 200 PC column). Some PrP^C preparations were digested with 2 units/ml endoglycosidase F (*Elizabethkingia meningoseptica*), 0.2 units/ml PI-PLC (*Bacillus cereus*), 10 units/ml bee venom PLA_2, or 0.2 units/ml neuraminidase (*Clostridium perfringens*) (all from Sigma) for 2 h at 37 °C. Samples were centrifuged through a 50-kDa filter to remove enzymes, and samples were loaded onto C18 columns (Waters). Proteins were purified using reverse phase chromatography with a gradient of propanol in water. Fractions were tested by ELISA; PrP-containing fractions were pooled, desalted, and stored at −80 °C. For bioassays, samples were thawed on the day of use and solubilized in culture medium by sonication.

PrP ELISA—The concentrations of PrP in samples were determined by ELISA as described (8). Briefly, Maxisorb immunoplates were coated with mAb ICSM18 and blocked with 5% milk powder. Samples were applied and detected with biotinylated mAb ICSM35, followed by extravidin-alkaline phosphatase and 1 mg/ml 4-nitrophenyl phosphate. Absorbance was measured on a microplate reader at 405 nm, and the amount of PrP in samples was calculated by reference to a standard curve of recombinant murine PrP (Fisher).

Isolation of CD14—CD14 was isolated from N9 glial cells that had been homogenized in an extraction buffer (as above). Insoluble debris and nuclei were removed by centrifugation. CD14 in the postnuclear supernatant was isolated using an affinity column loaded with rat anti-mouse CD14 mAb (clone RmC5-3) (BD Biosciences). CD14 was eluted with glycine-HCl at pH 2.7, neutralized with 1 M Tris, and loaded onto C18 columns. Proteins were eluted under a gradient of acetonitrile in water and 0.1% TFA. Fractions were tested by ELISA, and CD14-containing fractions were pooled, lyophilized, and stored at −80 °C. For bioassays, samples were thawed on the day of use and solubilized in culture medium by sonication.

CD14 ELISA—Concentrations of CD14 were measured by ELISA as described (39). Briefly, Maxisorb immunoplates were coated with 0.5 μg/ml rat IgG1 anti-mouse CD14 mAb (clone RmC5-3). Samples were applied, and bound CD14 was detected using a goat polyclonal IgG anti-mouse CD14 (R&D Systems), followed by anti-goat IgG conjugated to alkaline phosphatase

(Sigma) and 1 mg/ml 4-nitrophenyl phosphate. Absorbance was measured on a microplate reader at 405 nm and compared with a titration of recombinant mouse CD14 (Enzo Lifesciences).

Isolation and Analysis of GPI Anchors—PrP^C preparations were digested with 100 μg/ml proteinase K for 24 h at 37 °C, resulting in GPI anchors attached to the terminal amino acid. The released GPIs were extracted with water-saturated butan-1-ol and washed with water a further three times before being loaded onto C18 columns. GPIs were eluted using reverse phase chromatography under a gradient of acetonitrile and water. GPIs were detected by ELISA (see below), and positive fractions were pooled and lyophilized. Stock solutions were dissolved in ethanol at 2 μM. For some experiments, isolated GPIs were conjugated to FITC using the free amino group on the remaining amino acid and the homobifunctional cross-linking agent dimethyl pimelimidate (Fisher) using the manufacturer's instructions. Stock solutions were diluted in tissue culture medium for bioassays. GPIs were detected by immunoblotting as described with a mAb to phosphatidylinositol (34). The concentrations of FITC-labeled GPIs in samples were calculated by measuring fluorescence, excitation at 490 nm, and emission at 525 nm and compared with a dose response of FITC. Extracted GPIs were applied to silica gel 60 HPTLC plates (Whatman) and developed using a mixture of chloroform/methanol/water (4:4:1, v/v/v). Plates were soaked in 0.1% polyisobutyl methacrylate in hexane, dried, and blocked with 5% milk powder and probed with 1 μg/ml of mAb 5AB3-11, followed by biotinylated anti-mouse IgM and extravidin-horseradish peroxidase (Sigma), and visualized using chemiluminescence.

GPI ELISA—Maxisorb immunoplates were coated with 0.5 μg/ml concanavalin A (which binds mannose) and blocked with 5% milk powder in PBS-Tween. Samples were added, and any bound GPI was detected by the addition of the phosphatidylinositol-reactive mAb 5AB3-11, followed by a biotinylated anti-mouse IgM (Sigma), extravidin-alkaline phosphatase, and 1 mg/ml 4-nitrophenyl phosphate. Absorbance was measured at 405 nm.

Lectin Analysis of GPI Anchors—The presence of specific glycans in GPI anchors was determined using biotinylated lectins and dot blotting as described (34). Isolated GPIs were blotted onto nitrocellulose membranes, which were blocked (10% milk powder). Samples were incubated with biotinylated *S. nigra* (which detects terminal sialic acid residues bound α-2,6 or α-2,3 to galactose) or biotinylated concanavalin A to detect mannose (Vector Laboratories). Bound biotinylated lectins were visualized using extravidin peroxidase and enhanced chemiluminescence. The presence of phosphatidylinositol in GPIs was determined using mAb (5AB3-11), which was visualized using a horseradish peroxidase-conjugated anti-murine IgG and chemiluminescence.

Conjugation of GPIs to Rabbit IgG—Rabbit IgG (Sigma) was conjugated to GPIs by a two-step process. First, GPIs were conjugated to protein A (Innova Biosciences). The protein A complex was then cross-linked to rabbit IgG, and both steps used the homobifunctional cross-linking agent dimethyl pimelimidate (Pierce) according to the manufacturer's instructions. IgG-GPI conjugates were purified using reverse phase chromatography on C18 columns. The concentrations of rabbit IgG in samples were measured by ELISA. Maxisorb immunoplates were coated with mAb anti-rabbit IgG, clone L27A9 (New England Biolabs) and blocked with 5% milk powder. Samples were added, and rabbit IgG was detected with biotinylated goat anti-rabbit IgG (Sigma) followed by extravidin-alkaline phosphatase and 1 mg/ml 4-nitrophenyl phosphate. Absorbance was measured on a microplate reader at 405 nm, and the amount of rabbit IgG in samples was calculated by reference to a standard curve of rabbit IgG (Sigma). IgG and IgG-GPI conjugates were separated by HPTLC on silica gel 60 plates and developed using a mixture of chloroform/methanol/water (4:4:1, v/v/v).

Statistical Methods—Comparison of treatment effects was carried out using Student's paired *t* tests and one-way and two-way analysis of variance with Bonferroni's post hoc tests (IBM SPSS Statistics version 20). Error values are S.D., and significance was determined where p was <0.01. Correlations between data sets were analyzed using Pearson's bivariate coefficient (IBM SPSS Statistics version 20).

Author Contributions—C. B., W. N., and H. M.-O. were responsible for carrying out the experiments and data analysis. C. B. and A. W. were responsible for planning experiments and writing the manuscript.

References

1. Prusiner, S. B. (1998) Prions. *Proc. Natl. Acad. Sci. U.S.A.* **95,** 13363–13383
2. Herms, J., Tings, T., Gall, S., Madlung, A., Giese, A., Siebert, H., Schürmann, P., Windl, O., Brose, N., and Kretzschmar, H. (1999) Evidence of presynaptic location and function of the prion protein. *J. Neurosci.* **19,** 8866–8875
3. Brown, D. R. (2001) Prion and prejudice: normal protein and the synapse. *Trends Neurosci.* **24,** 85–90
4. Lledo, P. M., Tremblay, P., DeArmond, S. J., Prusiner, S. B., and Nicoll, R. A. (1996) Mice deficient for prion protein exhibit normal neuronal excitability and synaptic transmission in the hippocampus. *Proc. Natl. Acad. Sci. U.S.A.* **93,** 2403–2407
5. Maglio, L. E., Martins, V. R., Izquierdo, I., and Ramirez, O. A. (2006) Role of cellular prion protein on LTP expression in aged mice. *Brain Res.* **1097,** 11–18
6. Stahl, N., Borchelt, D. R., Hsiao, K., and Prusiner, S. B. (1987) Scrapie prion protein contains a phosphatidylinositol glycolipid. *Cell* **51,** 229–240
7. Taraboulos, A., Scott, M., Semenov, A., Avrahami, D., Laszlo, L., Prusiner, S. B., and Avraham, D. (1995) Cholesterol depletion and modification of COOH-terminal targeting sequence of the prion protein inhibit formation of the scrapie isoform. *J. Cell Biol.* **129,** 121–132
8. Bate, C., and Williams, A. (2011) Monoacylated cellular prion protein modifies cell membranes, inhibits cell signaling and reduces prion formation. *J. Biol. Chem.* **286,** 8752–8758
9. Puig, B., Altmeppen, H. C., Thurm, D., Geissen, M., Conrad, C., Braulke, T., and Glatzel, M. (2011) *N*-Glycans and glycosylphosphatidylinositol-anchor act on polarized sorting of mouse PrP(C) in Madin-Darby canine kidney cells. *PLoS One* **6,** e24624
10. Vey, M., Pilkuhn, S., Wille, H., Nixon, R., DeArmond, S. J., Smart, E. J., Anderson, R. G., Taraboulos, A., and Prusiner, S. B. (1996) Subcellular colocalization of the cellular and scrapie prion proteins in caveolae-like membranous domains. *Proc. Natl. Acad. Sci. U.S.A.* **93,** 14945–14949
11. Taylor, D. R., and Hooper, N. M. (2006) The prion protein and lipid rafts. *Mol. Membr. Biol.* **23,** 89–99
12. Pike, L. J. (2004) Lipid rafts: heterogeneity on the high seas. *Biochem. J.* **378,** 281–292
13. Madore, N., Smith, K. L., Graham, C. H., Jen, A., Brady, K., Hall, S., and Morris, R. (1999) Functionally different GPI proteins are organized in

different domains on the neuronal surface. *EMBO J.* **18,** 6917–6926
14. Ikezawa, H. (2002) Glycosylphosphatidylinositol (GPI)-anchored proteins. *Biol. Pharm. Bull.* **25,** 409–417
15. Stahl, N., Baldwin, M. A., Hecker, R., Pan, K. M., Burlingame, A. L., and Prusiner, S. B. (1992) Glycosylinositol phospholipid anchors of the scrapie and cellular prion proteins contain sialic acid. *Biochemistry* **31,** 5043–5053
16. Homans, S. W., Ferguson, M. A. J., Dwek, R. A., Rademacher, T. W., Anand, R., and Williams, A. F. (1988) Complete structure of the glycosyl phosphatidylinositol membrane anchor of rat brain Thy-1 glycoprotein. *Nature* **333,** 269–272
17. Premkumar, D. R., Fukuoka, Y., Sevlever, D., Brunschwig, E., Rosenberry, T. L., Tykocinski, M. L., and Medof, M. E. (2001) Properties of exogenously added GPI-anchored proteins following their incorporation into cells. *J. Cell Biochem.* **82,** 234–245
18. Zacharias, D. A., Violin, J. D., Newton, A. C., and Tsien, R. Y. (2002) Partitioning of lipid-modified monomeric GFPs into membrane microdomains of live cells. *Science* **296,** 913–916
19. Sunyach, C., Jen, A., Deng, J., Fitzgerald, K. T., Frobert, Y., Grassi, J., McCaffrey, M. W., and Morris, R. (2003) The mechanism of internalization of glycosylphosphatidylinositol-anchored prion protein. *EMBO J.* **22,** 3591–3601
20. Legler, D. F., Doucey, M. A., Schneider, P., Chapatte, L., Bender, F. C., and Bron, C. (2005) Differential insertion of GPI-anchored GFPs into lipid rafts of live cells. *FASEB J.* **19,** 73–75
21. Li, R., Liu, T., Yoshihiro, F., Tary-Lehmann, M., Obrenovich, M., Kuekrek, H., Kang, S.-C., Pan, T., Wong, B.-S., Medof, M. E., and Sy, M.-S. (2003) On the same cell type GPI-anchored normal cellular prion and DAF protein exhibit different biological properties. *Biochem. Biophys. Res. Commun.* **303,** 446–451
22. Liu, T., Li, R., Pan, T., Liu, D., Petersen, R. B., Wong, B. S., Gambetti, P., and Sy, M. S. (2002) Intercellular transfer of the cellular prion protein. *J. Biol. Chem.* **277,** 47671–47678
23. Bate, C., Salmona, M., Diomede, L., and Williams, A. (2004) Squalestatin cures prion-infected neurons and protects against prion neurotoxicity. *J. Biol. Chem.* **279,** 14983–14990
24. Gilch, S., Kehler, C., and Schätzl, H. M. (2006) The prion protein requires cholesterol for cell surface localization. *Mol. Cell Neurosci.* **31,** 346–353
25. Crick, D. C., Suders, J., Kluthe, C. M., Andres, D. A., and Waechter, C. J. (1995) Selective inhibition of cholesterol biosynthesis in brain cells by squalestatin 1. *J. Neurochem* **65,** 1365–1373
26. Hering, H., Lin, C. C., and Sheng, M. (2003) Lipid rafts in the maintenance of synapses, dendritic spines, and surface AMPA receptor stability. *J. Neurosci.* **23,** 3262–3271
27. Mauch, D. H., Nägler, K., Schumacher, S., Göritz, C., Müller, E.-C., Otto, A., and Pfrieger, F. W. (2001) CNS synaptogenesis promoted by glia-derived cholesterol. *Science* **294,** 1354–1357
28. Cancellotti, E., Wiseman, F., Tuzi, N. L., Baybutt, H., Monaghan, P., Aitchison, L., Simpson, J., and Manson, J. C. (2005) Altered glycosylated PrP proteins can have different neuronal trafficking in brain but do not acquire scrapie-like properties. *J. Biol. Chem.* **280,** 42909–42918
29. Tuzi, N. L., Cancellotti, E., Baybutt, H., Blackford, L., Bradford, B., Plinston, C., Coghill, A., Hart, P., Piccardo, P., Barron, R. M., and Manson, J. C. (2008) Host PrP glycosylation: a major factor determining the outcome of prion infection. *PLoS Biol.* **6,** e100
30. Haraguchi, T., Fisher, S., Olofsson, S., Endo, T., Groth, D., Tarentino, A., Borchelt, D. R., Teplow, D., Hood, L., and Burlingame, A. (1989) Asparagine-linked glycosylation of the scrapie and cellular prion proteins. *Arch. Biochem. Biophys.* **274,** 1–13
31. Chen, R., Walter, E. I., Parker, G., Lapurga, J. P., Millan, J. L., Ikehara, Y., Udenfriend, S., and Medof, M. E. (1998) Mammalian glycophosphatidylinositol anchor transfer to proteins and posttransfer deacylation. *Proc. Natl. Acad. Sci. U.S.A.* **95,** 9512–9517
32. McConville, M. J., and Ferguson, M. A. (1993) The structure, biosynthesis and function of glycosylated phosphatidylinositols in the parasitic protozoa and higher eukaryotes. *Biochem. J.* **294,** 305–324
33. Nicholson, T. B., and Stanners, C. P. (2006) Specific inhibition of GPI-anchored protein function by homing and self-association of specific GPI anchors. *J. Cell Biol.* **175,** 647–659
34. Bate, C., and Williams, A. (2012) Neurodegeneration induced by the clustering of sialylated glycosylphosphatidylinositols of prion proteins. *J. Biol. Chem.* **287,** 7935–7944
35. Maeda, Y., Tashima, Y., Houjou, T., Fujita, M., Yoko-o, T., Jigami, Y., Taguchi, R., and Kinoshita, T. (2007) Fatty acid remodeling of GPI-anchored proteins is required for their raft association. *Mol. Biol. Cell* **18,** 1497–1506
36. Schroeder, R., London, E., and Brown, D. (1994) Interactions between saturated acyl chains confer detergent resistance on lipids and glycosylphosphatidylinositol (GPI)-anchored proteins: GPI-anchored proteins in liposomes and cells show similar behavior. *Proc. Natl. Acad. Sci. U.S.A.* **91,** 12130–12134
37. Medof, M. E., Nagarajan, S., and Tykocinski, M. L. (1996) Cell-surface engineering with GPI-anchored proteins. *FASEB J.* **10,** 574–586
38. Anderson, R. G. W., and Jacobson, K. (2002) A role for lipid shells in targeting proteins to caveolae, rafts, and other lipid domains. *Science* **296,** 1821–1825
39. Ingham, V., Williams, A., and Bate, C. (2014) Glimepiride reduces CD14 expression and cytokine secretion from macrophages. *J. Neuroinflammation* **11,** 115
40. Brügger, B., Graham, C., Leibrecht, I., Mombelli, E., Jen, A., Wieland, F., and Morris, R. (2004) The membrane domains occupied by glycosylphosphatidylinositol-anchored prion protein and Thy-1 differ in lipid composition. *J. Biol. Chem.* **279,** 7530–7536
41. Bate, C., Nolan, W., and Williams, A. (2016) Sialic acid on the glycosylphosphatidylinositol anchor regulates PrP-mediated cell signaling and prion formation. *J. Biol. Chem.* **291,** 160–170
42. Cantù, L., Del Favero, E., Sonnino, S., and Prinetti, A. (2011) Gangliosides and the multiscale modulation of membrane structure. *Chem. Phys. Lipids* **164,** 796–810
43. Simons, M., Friedrichson, T., Schulz, J. B., Pitto, M., Masserini, M., and Kurzchalia, T. V. (1999) Exogenous administration of gangliosides displaces GPI-anchored proteins from lipid microdomains in living cells. *Mol. Biol. Cell* **10,** 3187–3196
44. Ohmi, Y., Ohkawa, Y., Yamauchi, Y., Tajima, O., Furukawa, K., and Furukawa, K. (2012) Essential roles of gangliosides in the formation and maintenance of membrane microdomains in brain tissues. *Neurochem. Res.* **37,** 1185–1191
45. Crespo, P. M., Zurita, A. R., and Daniotti, J. L. (2002) Effect of gangliosides on the distribution of a glycosylphosphatidylinositol-anchored protein in plasma membrane from Chinese hamster ovary-K1 cells. *J. Biol. Chem.* **277,** 44731–44739
46. Fujinaga, Y., Wolf, A. A., Rodighiero, C., Wheeler, H., Tsai, B., Allen, L., Jobling, M. G., Rapoport, T., Holmes, R. K., and Lencer, W. I. (2003) Gangliosides that associate with lipid rafts mediate transport of cholera and related toxins from the plasma membrane to endoplasmic reticulum. *Mol. Biol. Cell* **14,** 4783–4793
47. Galvan, C., Camoletto, P. G., Dotti, C. G., Aguzzi, A., and Ledesma, M. D. (2005) Proper axonal distribution of PrP^C depends on cholesterol-sphingomyelin-enriched membrane domains and is developmentally regulated in hippocampal neurons. *Mol. Cell Neurosci.* **30,** 304–315
48. Dunkley, P. R., Jarvie, P. E., and Robinson, P. J. (2008) A rapid Percoll gradient procedure for preparation of synaptosomes. *Nat. Protoc.* **3,** 1718–1728
49. London, E., and Brown, D. A. (2000) Insolubility of lipids in Triton X-100: physical origin and relationship to sphingolipid/cholesterol membrane domains (rafts). *Biochim. Biophys. Acta* **1508,** 182–195
50. Lipton, A. M., Cullum, C. M., Satumtira, S., Sontag, E., Hynan, L. S., White, C. L., 3rd, and Bigio, E. H. (2001) Contribution of asymmetric synapse loss to lateralizing clinical deficits in frontotemporal dementias. *Arch. Neurol.* **58,** 1233–1239

Sialic Acid within the Glycosylphosphatidylinositol Anchor Targets the Cellular Prion Protein to Synapses

Clive Bate, William Nolan, Harriet McHale-Owen and Alun Williams

J. Biol. Chem. 2016, 291:17093-17101.
doi: 10.1074/jbc.M116.731117 originally published online June 20, 2016